

Modelling of magnetic fields of CP stars

III. The combined interpretation of five different magnetic observables: theory, and application to β Coronae Borealis

S. Bagnulo¹, M. Landolfi², G. Mathys³, and M. Landi Degl'Innocenti⁴

¹ Universität Wien, Institut für Astronomie, Türkenschanzstrasse 17, 1180 Wien, Austria (bagnulo@astro.univie.ac.at)

² Osservatorio Astrofisico di Arcetri, Largo E. Fermi 5, 50125 Firenze, Italy (landolfi@arcetri.astro.it)

³ European Southern Observatory, Casilla 19001, Santiago 19, Chile (gmathys@eso.org)

⁴ C.N.R., Gruppo Nazionale di Astronomia, Unità di Ricerca di Arcetri, Largo E. Fermi 5, 50125 Firenze, Italy (mlandi@arcetri.astro.it)

Received 6 October 1999 / Accepted 2 February 2000

Abstract. The most common techniques for detecting magnetic fields of chemically peculiar (CP) stars are based on the determination of some quantities related to the magnetic morphology, which are obtained through the analysis of Stokes I and V profiles, and on observations of frequency integrated Stokes Q and U . In previous papers of this series we set up a formalism aimed at describing the magnetic field of CP stars in terms of a superposition of a dipole and a quadrupole field, and we proposed a method to recover the magnetic morphology from the combined analysis of those observable quantities which can simply be expressed by means of analytical formulas, namely: the mean longitudinal field, the crossover, and the mean square field. Here we extend this method in order to include those quantities for which numerical integrations are required, i.e., the mean field modulus and the broadband linear polarisation. Estimates of stellar radius and projected equatorial velocity are also explicitly taken into account. We present an application to the well-known CP star β CrB, the only star for which all kinds of magnetic data are available. We find that β CrB, like most CP stars, exhibits a complex magnetic structure, which may not be fully accounted for even by a second-order multipolar expansion. However, we are able to suggest two models which are compatible with all the magnetic data.

Key words: stars: magnetic fields – polarization – stars: chemically peculiar – stars: individual: β CrB

1. Introduction

Spectra of chemically peculiar (CP) stars of the upper main sequence exhibit a wealth of features uncommon to those of the majority of the objects located in the same region of the H-R diagram. Spectral lines of certain elements appear stronger, or weaker, than those of most of the stars of similar spectral type. In many cases, the spectral lines are polarised, and both shape and strength of the observed Stokes profiles change peri-

odically with time, with the same period as the light variations. These observations suggest that the photospheres of CP stars are characterised by non-cosmic element abundances, and that the regions of line formation are often permeated by a large-scale organised magnetic field (with a typical strength of few hundred to few ten thousand G). A magnetic morphology not symmetric around the rotation axis accounts for the periodic variation of the observed spectra, although, in some cases, abundance inhomogeneities must also be invoked to explain dramatic changes of the line strengths.

Abundance anomalies and presence of a magnetic field are correlated phenomena. Diffusing elements are guided by the magnetic field, some of them (like rare earths) may be concentrated where the field lines are horizontal, some others (e.g., Sr) where the field lines are vertical (Michaud et al. 1981). The situation is actually extremely complex, and predictions for diffusion of the various elements vary from star to star. It is clear that obtaining realistic models for the magnetic morphologies can provide very useful constraints to the diffusion theory, and can also help to understand the origin of the magnetic field in CP stars.

Although the signature of the Zeeman effect is quite clear in the observed spectra, it proves unpractical to try to recover the magnetic configuration via computation of straight fits to the observed spectra. The limited spectral resolution and signal-to-noise ratios that can be achieved in spectropolarimetric observations generally hamper the plain application of an inversion procedure, which they tend to render unstable. During the last years, however, a number of techniques have been introduced for measuring certain quantities related to the magnetic field, based on the combined use of the information contained in several spectral lines. Such quantities are usually determined with better accuracy, so that, at the moment, they look more adequate as diagnostic tools for recovering the magnetic configuration. This approach also has the advantage of being relatively independent of the various stellar parameters such as effective temperature, gravity and element abundances, and the inversion procedure does not require to perform time consuming spectral synthesis.

Send offprint requests to: S. Bagnulo

So far, four such quantities have been determined via the analysis of Stokes I and V line profiles, namely, *i*) the mean longitudinal field (e.g., Babcock 1947; Mathys 1991), *ii*) the crossover (Mathys 1995a), *iii*) the mean square field (Mathys 1995b), and *iv*) the mean field modulus (Babcock 1960; Mathys et al. 1997). Magnetic signatures in Stokes Q and U are considerably smaller than in Stokes I and V , so that noise limitations are even more penalising for the former two parameters than for the latter. As a result, the first unquestioned measurements of linear polarisation in spectral lines have been obtained in the last couple of years only, thanks to the combination of progress in the achievable quality of the observations and of new data analysis methods such as least-squares deconvolution (Wade et al. 1998) or the moment technique (Mathys 1999). Yet, such determinations are still too scarce to be useful for modelling purposes. By contrast, constraints to the magnetic field can be obtained via observations of broadband linear polarisation (BBLP) (e.g., Landi Degl'Innocenti et al. 1981; Landolfi et al. 1993a; Leroy 1995a).

The most favourable situation where all the magnetic quantities are well observed for one star is rarely encountered in real cases. This is partly due to intrinsic limits of the different observational techniques. Observations of magnetically split lines (from which one can derive the mean field modulus) are only possible for stars with small values of the projected equatorial velocity. On the other hand, for such stars observations of crossover (which is proportional to $v_e \sin i$) are unlikely to be significantly different from zero. Finally, observations of BBLP are only possible if the star's intrinsic signal is not washed out by interstellar polarisation: this limits the observations of BBLP to stars typically nearer than 100–200 pc. However, observations of all the five quantities mentioned above are available for one magnetic CP star (β CrB), and observations of three or four quantities are available for several others. Obviously, a reliable magnetic model should be able to account for *all* the different observables.

So far, most of the modelling was confined to one or two observable quantities, e.g., BBLP alone (Landolfi et al. 1993b), mean longitudinal field and mean field modulus (Hensberge et al. 1979; Wade et al. 1997), mean longitudinal field and BBLP (Bagnulo et al. 1995). More recently, Landolfi et al. (1998, hereafter referred to as Paper I) and Bagnulo et al. (1999a) tried to give a combined interpretation of three observational quantities (mean longitudinal field, crossover, and mean square field). In this paper we further generalise the technique proposed in Paper I in order to include the two remaining observables, BBLP and mean field modulus. Though straightforward in principle, such generalisation involves some technical difficulties that will be discussed in the following.

It has been known for a long time (e.g., Landstreet 1992) that the simple oblique rotator model with centred dipole field cannot explain the observations of magnetic CP stars in detail. The most direct extension of that model is the inclusion of a (non-linear) quadrupole contribution, which can be regarded as the first correction in the expansion of an arbitrary magnetic field into multipoles. The dipole plus quadrupole model has

already proved successful in several cases (Bagnulo et al. 1999a; Bagnulo & Landolfi 1999), so it has again been adopted in this paper.

As an application of the technique proposed in this paper, we present the results of the modelling of the magnetic CP star β CrB. For this star, two distinct dipole plus quadrupole models are found to be compatible with all the observational data. We present the corresponding magnetic maps, and discuss their reliability.

The paper is organised as follows. In Sect. 2 we give the explicit expressions for the BBLP and the mean field modulus. In Sect. 3 we outline the inversion procedure and we discuss which combinations of observable quantities are in principle sufficient to recover the magnetic configuration. In Sect. 4 we present the analysis of β CrB.

2. Expressions of the broadband linear polarisation and of the mean field modulus for the dipole plus quadrupole magnetic configuration

We assume that the magnetic configuration on the stellar surface is produced by the superposition of a dipole and a (non-linear) quadrupole located at the star's centre. The model is illustrated in Paper I; here we just recall the meaning of the different symbols, referring the reader to that paper for a detailed description of the magnetic geometry.

In the observer's reference frame (x, y, z) – see Fig. 1 of Paper I – the direction of the star's rotation axis is specified by two angles (inclination and azimuth) which are denoted by i and Θ respectively. The dipole is characterised by the amplitude B_d and by the unit vector $\mathbf{u} \equiv (\beta, f - f_0)$, where β is the angle between \mathbf{u} and the rotation axis and f is the rotational phase. Similarly, the quadrupole is characterised by the amplitude B_q and by the unit vectors $\mathbf{u}_1 \equiv (\beta_1, \gamma_1)$ and $\mathbf{u}_2 \equiv (\beta_2, \gamma_2)$. For an assigned magnetic configuration and an assigned value of the rotational phase, the magnetic field \mathcal{B} at the point $\mathbf{r} \equiv (R_*, \theta, \chi)$ of the stellar surface is given by the vector sum $\mathcal{B} = \mathcal{B}_d + \mathcal{B}_q$, where \mathcal{B}_d and \mathcal{B}_q are the dipole and quadrupole fields given by Eqs. (1) and (2), respectively, of Paper I. In the frame (x, y, z) the direction of $\mathcal{B}(\mathbf{r})$ is specified by the angles ψ and ϕ (see Fig. 1), which can easily be expressed in terms of the angles $i, \beta, f - f_0, \beta_1, \beta_2, \gamma_1, \gamma_2, \Theta, \theta, \chi$ (see below).

In Paper I we have introduced the quantities $F^{(1)}, F^{(2)}, F^{(3)}$ representing the mean longitudinal field, the crossover, and the mean square field respectively

$$\begin{aligned} F^{(1)} &= \langle \mathcal{B}_z \rangle \\ F^{(2)} &= v_e \sin i \langle d\mathcal{B}_z \rangle \\ F^{(3)} &= \langle \mathcal{B}^2 + \mathcal{B}_z^2 \rangle^{1/2}, \end{aligned} \quad (1)$$

where v_e is the star's equatorial velocity. They are functions of the rotational phase f and depend on the parameters specifying the magnetic configuration: their expressions for a dipole plus quadrupole field are given by Eqs. (4)-(7) of Paper I.

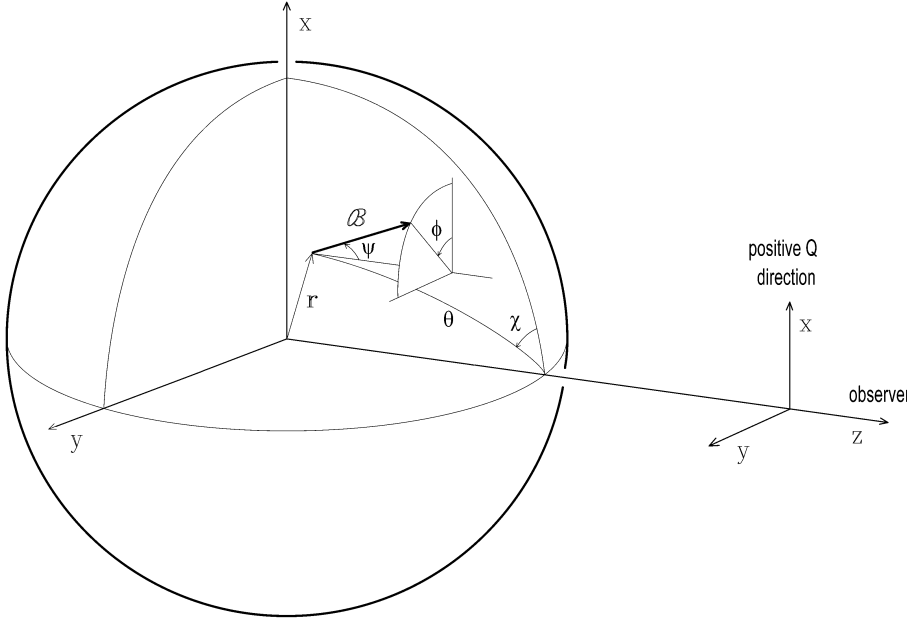


Fig. 1. In the observer's reference frame (x, y, z) the magnetic field vector \mathcal{B} at the point $\mathbf{r} \equiv (R_*, \theta, \chi)$ of the stellar surface is specified by the inclination angle ψ and the azimuth angle ϕ

Similarly, we now define the functions

$$\begin{aligned} F^{(4)} &= P_Q + P_Q^{\text{int}} \\ F^{(5)} &= P_U + P_U^{\text{int}} \\ F^{(6)} &= \langle \mathcal{B} \rangle, \end{aligned} \quad (2)$$

where P_Q, P_U are the disk averages of the Stokes parameters Q, U integrated in frequency across a given interval $\Delta\nu$ and normalised to the intensity flux in the same interval, $P_Q^{\text{int}}, P_U^{\text{int}}$ are the contributions to these quantities due to interstellar polarisation, and $\langle \mathcal{B} \rangle$ is the mean field modulus. We want to establish the expressions of $F^{(4)}, F^{(5)}, F^{(6)}$ for the dipole plus quadrupole magnetic configuration.

Consider first the quantities P_Q, P_U (i.e., the BBLP). We have by definition

$$\begin{aligned} P_Q &= \frac{\int_0^{2\pi} d\chi \int_0^{\pi/2} d\theta \sin\theta \cos\theta \int_{\Delta\nu} d\nu Q_\nu(\theta, \chi)}{\int_0^{2\pi} d\chi \int_0^{\pi/2} d\theta \sin\theta \cos\theta \int_{\Delta\nu} d\nu I_\nu(\theta, \chi)} \\ P_U &= \frac{\int_0^{2\pi} d\chi \int_0^{\pi/2} d\theta \sin\theta \cos\theta \int_{\Delta\nu} d\nu U_\nu(\theta, \chi)}{\int_0^{2\pi} d\chi \int_0^{\pi/2} d\theta \sin\theta \cos\theta \int_{\Delta\nu} d\nu I_\nu(\theta, \chi)}, \end{aligned} \quad (3)$$

where I_ν, Q_ν, U_ν are the Stokes parameters (hereafter defined as in Shurcliff 1962) of the radiation of frequency ν coming from the point \mathbf{r} .

Our basic assumption is that the BBLP actually observed in several CP stars (see Leroy 1995a for a comprehensive presentation of measurements) is due to the differential saturation mechanism. According to this mechanism – first introduced by Leroy (1962) to interpret the BBLP observed in sunspots – the polarisation results from the cumulative effect of all the magnetically sensitive lines contained in the observed spectral interval. The contribution of each single line arises from the combination of two effects: the splitting (due to the presence of a magnetic

field) and the saturation (due to the transfer of radiation) which is generally different for σ and π Zeeman components. Since both effects are obviously present in the atmosphere of a magnetic CP star, it looks quite natural to ascribe the observed BBLP to such a mechanism. This approach has been followed in several works (e.g., Landi Degl'Innocenti et al. 1981; Landolfi et al. 1993a,b; Bagnulo et al. 1995).

Then we assume that the element abundances on the stellar surface are constant, and that N identical, well-separated (unblended) lines are contained in the interval $\Delta\nu$: in other words, we assume that the observed BBLP is produced by an ‘average’ line, whose properties are the same throughout the whole surface.

The above assumptions allow us to replace in Eqs. (3)

$$\begin{aligned} \int_{\Delta\nu} d\nu Q_\nu(\theta, \chi) &\rightarrow N \int_{\text{line}} d\nu Q_\nu(\theta, \chi) \\ \int_{\Delta\nu} d\nu U_\nu(\theta, \chi) &\rightarrow N \int_{\text{line}} d\nu U_\nu(\theta, \chi) \\ \int_{\Delta\nu} d\nu I_\nu(\theta, \chi) &\rightarrow \int_{\Delta\nu} d\nu I_c(\theta, \chi) \\ &\quad - N \int_{\text{line}} d\nu [I_c(\theta, \chi) - I_\nu(\theta, \chi)], \end{aligned} \quad (4)$$

where I_c is the continuum intensity and *line* means that the integrals extend over the profile of the ‘average’ line.

Finally, we assume that the atmosphere is described by the Milne-Eddington model, which implies that the Stokes parameters of the emitted radiation are given by the well-known Unno-Rachkovsky formulas. However, in accordance with Paper I, we replace the limb-darkening law in $\cos\theta$ with the more realistic law $(1 - u + u \cos\theta)$. Thus we use the expressions

$$\begin{aligned} I_\nu(\theta, \chi) &= B_0 + (1 - u + u \cos\theta) B_1 i(\theta, \chi) \\ Q_\nu(\theta, \chi) &= -(1 - u + u \cos\theta) B_1 q(\theta, \chi) \\ U_\nu(\theta, \chi) &= -(1 - u + u \cos\theta) B_1 u(\theta, \chi), \end{aligned} \quad (5)$$

where B_0 and B_1 characterize the dependence of the Planck function B_P on optical depth ($B_P(\tau) = B_0 + B_1\tau$), and where

$$\begin{aligned} i(\theta, \chi) &= \Delta^{-1}(1 + \eta_I)[(1 + \eta_I)^2 + \rho_Q^2 + \rho_U^2 + \rho_V^2] \\ q(\theta, \chi) &= \Delta^{-1}[(1 + \eta_I)^2\eta_Q + (1 + \eta_I)(\eta_V\rho_U - \eta_U\rho_V) \\ &\quad + \rho_Q(\eta_Q\rho_Q + \eta_U\rho_U + \eta_V\rho_V)] \\ u(\theta, \chi) &= \Delta^{-1}[(1 + \eta_I)^2\eta_U + (1 + \eta_I)(\eta_Q\rho_V - \eta_V\rho_Q) \\ &\quad + \rho_U(\eta_Q\rho_Q + \eta_U\rho_U + \eta_V\rho_V)], \end{aligned} \quad (6)$$

with

$$\begin{aligned} \Delta &= (1 + \eta_I)^2 \\ &\quad \times [(1 + \eta_I)^2 - \eta_Q^2 - \eta_U^2 - \eta_V^2 + \rho_Q^2 + \rho_U^2 + \rho_V^2] \\ &\quad - (\eta_Q\rho_Q + \eta_U\rho_U + \eta_V\rho_V)^2. \end{aligned}$$

The quantities $\eta_{I,Q,U,V}$ and $\rho_{Q,U,V}$ have their usual meaning (see e.g. Landolfi & Landi Degl'Innocenti 1982). Since they depend on ν via the reduced frequency

$$v = (\nu_0 - \nu)/\Delta\nu_D, \quad (7)$$

where ν_0 is the line centre frequency and $\Delta\nu_D$ the Doppler width, it is convenient to change the integration variable in Eqs. (4) from ν to v . From Eqs. (2)-(5) we finally obtain

$$\begin{aligned} F^{(4)} &= -\frac{\alpha \int_0^{2\pi} d\chi \int_0^{\pi/2} d\theta c(\theta;u) \int_{\text{line}} dv q(\theta,\chi)}{1 - \alpha \int_0^{2\pi} d\chi \int_0^{\pi/2} d\theta c(\theta;u) \int_{\text{line}} dv [1 - i(\theta,\chi)]} + P_Q^{\text{int}} \\ F^{(5)} &= -\frac{\alpha \int_0^{2\pi} d\chi \int_0^{\pi/2} d\theta c(\theta;u) \int_{\text{line}} dv u(\theta,\chi)}{1 - \alpha \int_0^{2\pi} d\chi \int_0^{\pi/2} d\theta c(\theta;u) \int_{\text{line}} dv [1 - i(\theta,\chi)]} + P_U^{\text{int}}, \end{aligned} \quad (8)$$

where

$$c(\theta; u) = \sin \theta \cos \theta (1 - u + u \cos \theta) \quad (9)$$

and

$$\alpha = \frac{N \Delta\nu_D \beta_P}{\pi \Delta\nu [1 + \frac{3-u}{3} \beta_P]}, \quad (10)$$

with $\beta_P = B_1/B_0$.

In several previous papers dealing with the interpretation of BBLP observations in CP stars, the so-called weak field approximation has been used. This approximation entails a major simplification, because it allows one to evaluate analytically the disk integrals appearing in Eqs. (8). Such calculations have been carried out in Landolfi et al. (1993a) for the dipole field (and a special type of dipole plus quadrupole, the quadrupole being linear and aligned with the dipole), and in Bagnulo et al. (1996) for an arbitrary multipole field. In the former paper, and in Bagnulo et al. (1995), it was shown that the weak field approximation does not introduce large errors for the magnetic configurations considered, up to field strengths of about 20 kG. At the same time, it was suggested that this property (which is not obvious, since the weak field approximation is verified, in metallic lines, for a strength up to $\simeq 1$ kG) is most likely related to the fact that, for those configurations, the variation of the field modulus across the stellar surface is small. This is *not* the case, however,

for the superposition of a dipole and a non-linear quadrupole. In fact we found, by comparing the polarisation predicted by Eqs. (8) and by the analytical expressions given in Bagnulo et al. (1996), that the weak field approximation is *not* adequate for the dipole plus non-linear quadrupole configuration considered in the present paper. Hence we are forced to give up this approximation, and to evaluate numerically the integrals in Eqs. (8).

The quantities $\eta_{I,Q,U,V}$ and $\rho_{Q,U,V}$ depend on the strength η_0 and on the damping constant a of the 'average' line. Furthermore they depend on the magnetic field vector $\mathcal{B}(\mathbf{r})$ via the Zeeman splitting normalised to the Doppler width¹

$$v_H = \mathcal{B}/b \quad (11)$$

with

$$b = \frac{4\pi mc \Delta\nu_D}{eg} \quad (12)$$

(where g is the Landé factor of the line and e, m, c the electron charge and mass and the velocity of light, respectively), and via the angular factors $\sin^2\psi \cos 2\phi$, $\sin^2\psi \sin 2\phi$, $\cos\psi$, where ψ and ϕ are the angles defined in Fig. 1. Such quantities can easily be expressed in terms of the components of \mathcal{B} in the reference frame (x, y, z)

$$\begin{aligned} \mathcal{B} &= \sqrt{\mathcal{B}_x^2 + \mathcal{B}_y^2 + \mathcal{B}_z^2} \\ \sin^2\psi \cos 2\phi &= (\mathcal{B}_x^2 - \mathcal{B}_y^2)/\mathcal{B}^2 \\ \sin^2\psi \sin 2\phi &= 2\mathcal{B}_x\mathcal{B}_y/\mathcal{B}^2 \\ \cos\psi &= \mathcal{B}_z/\mathcal{B}. \end{aligned} \quad (13)$$

The components $\mathcal{B}_x, \mathcal{B}_y, \mathcal{B}_z$ can in turn be calculated from Eqs. (1) and (2) of Paper I once the components of the unit vectors $\mathbf{u}, \mathbf{u}_1, \mathbf{u}_2$ in the frame (x, y, z) are known. Denoting such components by $(X, Y, Z), (X_1, Y_1, Z_1), (X_2, Y_2, Z_2)$ respectively, we have (cf. Eqs. (30) of Bagnulo et al. 1996 and Eqs. (7) of Paper I)²

$$\begin{aligned} X &= \cos \Theta [\sin i \cos \beta \\ &\quad - \cos i \sin \beta \cos(f - f_0)] \\ &\quad + \sin \Theta \sin \beta \sin(f - f_0) \\ X_\ell &= \cos \Theta [\sin i \cos \beta_\ell \\ &\quad - \cos i \sin \beta_\ell \cos(f - f_0 + \gamma_\ell)] \\ &\quad + \sin \Theta \sin \beta_\ell \sin(f - f_0 + \gamma_\ell) \\ Y &= \sin \Theta [\sin i \cos \beta \\ &\quad - \cos i \sin \beta \cos(f - f_0)] \\ &\quad - \cos \Theta \sin \beta \sin(f - f_0) \\ Y_\ell &= \sin \Theta [\sin i \cos \beta_\ell \\ &\quad - \cos i \sin \beta_\ell \cos(f - f_0 + \gamma_\ell)] \\ &\quad - \cos \Theta \sin \beta_\ell \sin(f - f_0 + \gamma_\ell) \\ Z &= \cos i \cos \beta + \sin i \sin \beta \cos(f - f_0) \\ Z_\ell &= \cos i \cos \beta_\ell + \sin i \sin \beta_\ell \cos(f - f_0 + \gamma_\ell), \end{aligned} \quad (14)$$

with $\ell = 1, 2$.

¹ For simplicity, the 'average' line is assumed to be a Zeeman triplet.

² We recall that, contrary to the functions $F^{(1)}, F^{(2)}, F^{(3)}$ and $F^{(6)}$, the BBLP also depends on the angle Θ .

It should be noticed that the denominator of the first terms in the r.h.s. of Eqs. (8) can be written in the form $(1 - \xi)$, where ξ is the line-blocking factor representing the fraction of continuum radiation subtracted by the spectral lines contained in the interval $\Delta\nu$,

$$\xi = (F_c - F_I)/F_c, \quad (15)$$

where F_I and F_c are the fluxes

$$\begin{aligned} F_I &= \int_0^{2\pi} d\chi \int_0^{\pi/2} d\theta \sin \theta \cos \theta \int_{\Delta\nu} d\nu I_\nu(\theta, \chi) \\ F_c &= \int_0^{2\pi} d\chi \int_0^{\pi/2} d\theta \sin \theta \cos \theta \int_{\Delta\nu} d\nu I_c(\theta, \chi). \end{aligned} \quad (16)$$

Owing to magnetic intensification, ξ varies with the rotational phase f because the magnetic configuration on the visible hemisphere changes. Such variation has usually been neglected (see, e.g., Landi Degl'Innocenti et al. 1981; Landolfi et al. 1993a). Although it is not expected to affect deeply the BBLP signal (Leroy et al. 1995), in this paper we take it explicitly into account, in order to minimize the number of approximations.

The expression of the function $F^{(6)}$, the mean field modulus, is much more direct. From Eqs. (3), (4), (7) of Bagnulo et al. (1996) we have

$$\begin{aligned} F^{(6)} &= \frac{3}{\pi(3-u)} \\ &\times \int_0^{2\pi} d\chi \int_0^{\pi/2} d\theta c(\theta; u) \sqrt{\mathcal{B}_x^2 + \mathcal{B}_y^2 + \mathcal{B}_z^2}, \end{aligned} \quad (17)$$

where $c(\theta; u)$ is defined in Eq. (9). As noticed in that paper, the integral has to be evaluated numerically. For a given magnetic configuration and rotational phase, the components \mathcal{B}_x , \mathcal{B}_y , \mathcal{B}_z can be calculated as illustrated above.

It is thus seen that, when the dipole plus non-linear quadrupole configuration is considered, a common feature of the BBLP and the mean field modulus is that both require the numerical evaluation of certain integrals – contrary to the functions $F^{(1)}$, $F^{(2)}$, $F^{(3)}$ for which simple analytical expressions have been worked out. This is an obvious drawback from a practical point of view, when real observational data are to be interpreted.

3. The inversion procedure

Once the expressions of the quantities $F^{(k)}$ (with $k = 1, \dots, 6$) are established, we can try to interpret simultaneously all the different kinds of measurement available for a given star in terms of the dipole plus quadrupole magnetic model. It is however convenient to introduce, as further constraints to the fit, the values of the stellar radius R_* (which can always be estimated within some uncertainty) and – when known from Doppler broadening measurements – the projected equatorial velocity $v_e \sin i$. We recall that R_* is related to the rotation period P and the equatorial velocity v_e by $R_* = Pv_e/(2\pi)$. It has been shown (Bagnulo & Landolfi 1999) that inclusion of these constraints may help in discriminating among several possible models.

The search for the best model can be carried out by looking for the minimum, in the parameters space, of a χ^2 of the form

$$\begin{aligned} \chi^2 &= \sum_{k=1}^6 \sum_{i=1}^{n_k} \frac{\left[F_i^{(k)} - F^{(k)}(t_i^{(k)}) \right]^2}{\left[\sigma_i^{(k)} \right]^2} \\ &+ \frac{\left[R_*^{(0)} - R_* \right]^2}{\left[\sigma_{R_*} \right]^2} + \frac{\left[v_e \sin i^{(0)} - v_e \sin i \right]^2}{\left[\sigma_{v_e \sin i} \right]^2}, \end{aligned} \quad (18)$$

where $F_i^{(k)}$ are the measurements of the k^{th} observable (performed at times $t_i^{(k)}$, i.e. at rotational phases $f_i^{(k)} = f_0 + 2\pi t_i^{(k)}/P$), $R_*^{(0)}$ and $v_e \sin i^{(0)}$ the estimated/measured values of the stellar radius and the projected equatorial velocity, and σ the corresponding errors. The functions $F^{(1)}$, $F^{(2)}$, $F^{(3)}$ are given by Eqs. (4) of Paper I, the functions $F^{(4)}$, $F^{(5)}$, $F^{(6)}$ by Eqs. (8) and (17) of this paper.

When the observations of a given star are to be interpreted, it is appropriate to look both for the best dipole plus quadrupole model and for the best pure dipole model. In the latter case, the expressions of the functions $F^{(k)}(f)$ are readily obtained by neglecting, in the general expressions established above, all the terms involving B_q . The χ^2 defined in Eq. (18) depends on the parameters

$$i, \beta, f_0, B_d, v_e, \alpha, \Theta, P_Q^{\text{int}}, P_U^{\text{int}} \quad (19)$$

for the pure dipole configuration, and

$$i, \beta, \beta_1, \beta_2, f_0, \gamma_1, \gamma_2, B_d, B_q, v_e, \alpha, \Theta, P_Q^{\text{int}}, P_U^{\text{int}} \quad (20)$$

for the dipole plus quadrupole configuration. The last four parameters of each set are only present when BBLP measurements are included.

We developed two distinct codes for the search of the χ^2 minimum in the pure dipole and the dipole plus quadrupole case. These codes, which are based on the Marquardt algorithm (described, e.g., in Bevington 1969), are a direct generalisation of the codes illustrated in Paper I to include BBLP and mean field modulus observations (as well as the values of R_* and $v_e \sin i$). The same general remarks about the fitting method (including the existence of ‘unphysical’ sets of parameters and of relative minima on the χ^2 hypersurface) apply here as well. Obviously, the new codes require a much longer execution time because of the numerical evaluation of the integrals in Eqs. (8) and (17). We recall that the rotation period P and the limb-darkening coefficient u are treated as fixed parameters. We also recall, from the preceding section, that the BBLP depends on the additional parameters η_0 and a (the strength and damping constant of the ‘average’ line) and on the quantity b (having dimensions of magnetic field) defined in Eq. (12). Such quantities are also treated as fixed data, to avoid an exceedingly large number of free parameters. When BBLP observations are present, the fitting procedure is repeated for different values of η_0 , a , b (chosen within a physically reasonable range, see Sect. 4) until the absolute minimum of χ^2 is reached.

In principle, the method presented in this paper allows one to recover the magnetic configuration of a given star by using *any*

combination of observables (e.g. longitudinal field and BBLP, field modulus and $v_e \sin i$, BBLP alone, etc.). On the other hand, it is well-known that the knowledge of certain observables is not sufficient (whatever the precision and the phase coverage of the measurements) to recover the configuration: for example, even the pure dipole configuration cannot be retrieved from longitudinal field measurements alone. Therefore, the question arises as to which combinations of observables are in principle sufficient to recover the magnetic configuration.

A related question concerns the uniqueness of the recovered configuration. All the functions $F^{(k)}$ are, to some extent, invariant under certain transformations of the angles listed in Eqs. (19) and (20). Hence, according to the specific combination of observables considered, the recovered configuration will be more or less degenerate.³

The answer to such questions can be obtained by inspection of the expressions for the functions $F^{(k)}$, and can easily be checked via numerical simulations with the two codes mentioned above. The results are summarised in Table 1.

Consider first the pure dipole configuration. We label the degenerate magnetic configurations by the letters A through E according to the following scheme:

A_1 — unique configuration (no degeneracy);

B_1 — unique configuration (see below);

C_2 — two different configurations characterised by exchanged values for i and β (cf. Paper I, line d of Table 1):

$$(i, \beta, f_0),$$

$$(\beta, i, f_0);$$

D_2 — two different configurations characterised by the reversed direction of the magnetic field vector at any point of the stellar surface (cf. Paper I, line b of Table 1):

$$(i, \beta, f_0),$$

$$(i, \pi - \beta, \pi + f_0);$$

E_4 — four different configurations resulting from the combination of C_2 and D_2 :

$$(i, \beta, f_0), (\beta, i, f_0);$$

$$(i, \pi - \beta, \pi + f_0), (\beta, \pi - i, \pi + f_0).$$

Furthermore, in case A_1 both the star's rotation direction (clockwise or counterclockwise) and the azimuth Θ of the projected rotation axis are univocally determined (except for the ambiguity between Θ and $\Theta + \pi$), whereas in cases B_1 , C_2 , D_2 , E_4 both are undetermined.⁴

³ Contrary to Paper I, in the following analysis we disregard the 'pseudo-degeneracies' arising from the exchange of the unit vectors \mathbf{u}_1 , \mathbf{u}_2 and from the inversion of their directions, since both transformations leave the magnetic configuration unchanged.

⁴ The functions $F^{(1)}$, $F^{(2)}$, $F^{(3)}$, $F^{(6)}$ are both independent of Θ and invariant under the transformation ($i \rightarrow \pi - i, \beta \rightarrow \pi - \beta$), which describes two stars having the same magnetic configuration and rotating in opposite directions (cf. Paper I, line a of Table 1).

Table 1. The different combinations of observable quantities sufficient to recover the magnetic configuration, and the corresponding degeneracy

$F^{(1)}$	$F^{(2)}$	$F^{(3)}$	$F^{(4,5)}$	$F^{(6)}$	$v_e \sin i$	d	d + q
			*			A_1	A'_1
*							
	*						
		*				E_4	
				*		E_4	
*					*	B_1	
	*				*		
		*			*	D_2	
				*	*	D_2	C'_4
*	*						
*		*				C_2	B'_2
*				*		C_2	B'_2
	*	*				C_2	B'_2
	*			*		C_2	B'_2
		*		*		E_4	C'_4
*	*				*	B_1	
*		*			*	B_1	B'_2
*				*	*	B_1	B'_2
	*	*			*	B_1	B'_2
	*			*	*	B_1	B'_2
		*		*	*	D_2	C'_4
*	*	*				C_2	B'_2
*	*			*		C_2	B'_2
*		*		*		C_2	B'_2
	*	*		*		C_2	B'_2
*	*	*			*	B_1	B'_2
*	*			*	*	B_1	B'_2
*		*		*	*	B_1	B'_2
	*	*		*	*	B_1	B'_2
*	*	*		*		C_2	B'_2
*	*	*		*	*	B_1	B'_2

For the dipole plus quadrupole configuration we label the degenerate magnetic configurations as follows:

A'_1 — unique configuration (including the star's rotation direction and the angle Θ as in case A_1);

B'_2 — two different configurations, symmetrical about the plane containing the dipole axis and the rotation axis (cf. Paper I, line a of Table 3):

$$(i, \beta, \beta_1, \beta_2, f_0, \gamma_1, \gamma_2),$$

$$(\pi - i, \pi - \beta, \pi - \beta_1, \pi - \beta_2, f_0, \gamma_1, \gamma_2);$$

C'_4 — four different configurations resulting from combining B'_2 with the reversed direction of the magnetic field vector at any point of the stellar surface (cf. Paper I, line b_1 of Table 3):

$$\begin{aligned} & (i, \quad \beta, \quad \beta_1, \quad \beta_2, \quad f_0, \quad \gamma_1, \quad \gamma_2), \\ & (\pi - i, \pi - \beta, \pi - \beta_1, \pi - \beta_2, f_0, \gamma_1, \gamma_2), \\ & (i, \quad \pi - \beta, \beta_1, \quad \pi - \beta_2, \pi + f_0, \pi + \gamma_1, \gamma_2), \\ & (\pi - i, \quad \beta, \quad \pi - \beta_1, \quad \beta_2, \quad \pi + f_0, \pi + \gamma_1, \gamma_2). \end{aligned}$$

In Table 1, an asterisk means that the corresponding observable is known, an empty space that it is not known. The two last columns show the kind of degeneracy according to the preceding schemes, for the pure dipole (d) and the dipole plus quadrupole (d+q) configuration, respectively; an empty space in these columns means that the knowledge of the associated observable(s) is *not* sufficient to recover the configuration.

In the dipole case, it appears that the BBLP, the mean square field and the mean field modulus are sufficient by themselves to retrieve the magnetic configuration; the mean longitudinal field is sufficient only if $v_e \sin i$ is known. By contrast, the crossover is not sufficient, even if combined with $v_e \sin i$ or the longitudinal field. The only observable which enables one to determine univocally the configuration is the BBLP; obviously, any combination of observables which includes the BBLP has the same property (such combinations are not shown in Table 1). Omitting the BBLP, the number of degenerate configurations obviously decreases (changing from E_4 to C_2/D_2 and to B_1) as the number of known observables is increased; in particular, kind B_1 can only be obtained if $v_e \sin i$ is known.

Similar remarks apply to the dipole plus quadrupole case. The minimum combinations of observables sufficient to recover the magnetic configuration are: the BBLP by itself; the mean field modulus provided $v_e \sin i$ is known; any two observables among the longitudinal field, crossover, square field and field modulus (even if $v_e \sin i$ is not known), except longitudinal field and crossover: this combination is not sufficient even if $v_e \sin i$ is known.

Altogether, the BBLP turns out to be the richest in diagnostic content, the crossover the poorest. This does not mean that the actual localisation of the χ^2 minimum is easier when BBLP measurements are available: in fact the opposite is usually true, as expected because of the larger number of free parameters involved, which implies a more complex structure of the χ^2 hypersurface.

4. Application: Modelling of the magnetic field of β Coronae Borealis

4.1. Observations

β CrB (= HD 137909) is one of the best observed CP stars, and measurements of magnetic field have been performed by several authors. As for the mean longitudinal field, a list of references is given in Mathys (1991); for the mean field modulus, see Mathys et al. (1997). In this work we considered 21 determinations of mean longitudinal field, crossover, and mean square field, 46 determinations of mean field modulus, and 27 observations of

BBLP. Part of the determinations of longitudinal field, crossover and square field were published by Mathys (1994, 1995a) and Mathys & Hubrig (1997), while 32 determinations of field modulus were presented by Mathys et al. (1997). Work in progress by Mathys led to the revision of his earlier determinations of the square field (Mathys 1995b); these revised values are used here. The remaining measurements of all 4 quantities will be reported in Mathys et al. (in preparation). Finally, all the observations of BBLP, obtained in a 100 Å band centred at 4200 Å, were taken by Leroy (1995a).

It should be noted that measurements of longitudinal field carried out by other authors show discrepancies with the dataset that we have adopted for this analysis. As pointed out in Mathys (1991), other authors (e.g., Babcock 1958; Preston & Sturch 1967; Borra & Landstreet 1980) measured a weaker magnetic minimum than exhibited by our dataset, whereas Vogt et al. (1980) observed a magnetic minimum about 200 G more negative.

Longitudinal field determinations by Mathys (1994) rest on the analysis of spectral lines between 5800 and 6400 Å, a large fraction of which are located bluewards of 6000 Å, Vogt et al.'s (1980) work is based on observations at 6000–6100 Å, while almost all other determinations of longitudinal field are obtained from observations in the blue spectral region. Exceptions are the works of Wolff (1978) and Romanyuk (1986), who in fact performed a comparison of the curves of longitudinal field as obtained from observations on either side of the Balmer jump. Their results show that a systematic difference between the determinations of the longitudinal field obtained in the two different spectral regions may indeed be suspected, although the observed differences are probably smaller than the uncertainties inherent in the measurements.

Observations performed at different wavelengths imply a different sampling in depth of the stellar photosphere, and one may suspect that the field strength varies with depth, as already suggested by Wolff (1978) and Leroy (1995b).

The quality of the currently available observations is probably not sufficient to confirm whether this phenomenon is real, and dealing with a depth-dependent magnetic structure is out of the scope of the present modelling. In this paper we implicitly assume that discrepancies among different datasets are due to systematic effects introduced by the different observing techniques. The choice of Mathys (1994) dataset is almost mandatory for the sake of consistency with the available determinations of crossover and square field, which are performed on the same spectra used for the determinations of longitudinal field. Furthermore, this dataset is based on spectra obtained with an instrument (CASPEC) mounted at the Cassegrain focus, hence devoid of significant instrumental polarisation. By contrast, most other works are based on Coudé spectra, and the required compensation for instrumental polarisation is a source of uncertainty. This may be particularly critical and delicate for β CrB, as illustrated by the shift between the mean field modulus curves obtained from KPNO and AURELIE spectra reported in Mathys et al. (1997) (see also Fig. 2).

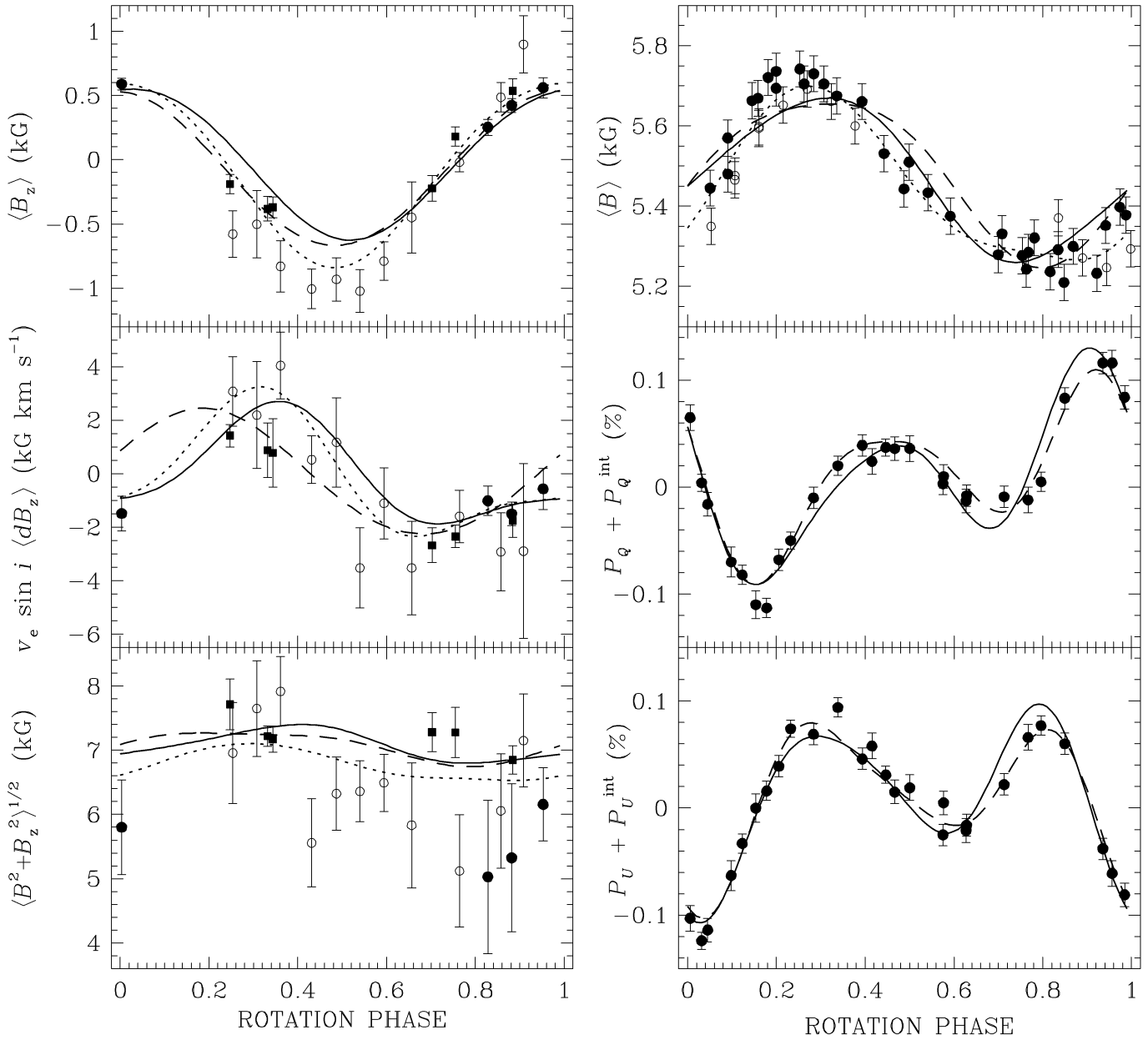


Fig. 2. The best-fits to the curves of longitudinal field, crossover, square field, field modulus, and BBLP (as customary, the so-called quadratic field $\sqrt{F^{(3)}}$ is shown in the place of $F^{(3)}$). Dotted lines show the best-fits obtained by neglecting the observations of BBLP. The dashed lines refer to the model of Eq. (22), the solid lines to the model of Eq. (23). Different symbols are used to distinguish various sets of measurements, between which systematic differences exist (see the references with the original measurements for details). In the left three panels, open circles correspond to the data from Mathys (1994, 1995a, 1995b), filled circles to those from Mathys & Hubrig (1997), and filled squares to those from Mathys et al. (in preparation). (In fact, early determinations of the mean square field were revised as explained in the text.) In the upper right panel, data obtained at Haute-Provence Observatory with the AURELIE spectrograph are represented by filled circles, and data obtained at Kitt Peak National Observatory with the cross-dispersed echelle spectrograph by open circles (see Mathys et al. 1997 for details)

β CrB is known as a binary, both by spectroscopy and speckle interferometry. According to Tokovinin (1985) its companion is 1.7 mag fainter in the V filter. For the stellar temperatures North et al. (1998) estimate $T_{\text{eff}} = 7750$ K and 7200 K, where the lower temperature refers to the fainter component, which in the following we will assume to be non-magnetic. According to these estimates, the contribution of the fainter com-

ponent to the observed flux in the visible is five times weaker than that due to the magnetic star. Close inspection of the spectra obtained at various orbital phases does not reveal any evidence of significant contribution of the lines of the secondary to the profiles of the diagnostic lines of the primary. Accordingly, the moments of those lines, and the magnetic quantities derived from their measurements, are unaffected by the fact that β CrB

is a binary system. The impact of the presence of a companion on the interpretation of the observations of BBLP will be discussed in Sect. 4.3.

For the rotation period we adopted the value of 18.4866 ± 0.001 d, which was derived via a Fourier analysis of the measurements of longitudinal field, field modulus, and BBLP. As constraint to the stellar radius we adopted the value $R_*^{(0)} = 3.25 \pm 0.31 R_\odot$, obtained from Hipparcos astrometry by Hubrig et al. (2000), whereas for the projected equatorial velocity we adopted the value $v_e \sin i^{(0)} = 3.5 \pm 1.5 \text{ km s}^{-1}$ given by Wade (1996). For the limb-darkening coefficient we adopted $u = 0.5$. This choice is not particularly crucial, since the observable quantities do not strongly depend on it: this was verified *a posteriori* by repeating the calculations with $u = 0.3$ and $u = 0.7$: the results were found to be consistent within the parameter errors.

4.2. Analysis

As explained in Sect. 3, a magnetic model for the star could be derived by the analysis of several different subsets of observable quantities (see Table 1). However, this possibility is effective only for data which are *exactly* measured, and the problem of the actual invertibility of the observations should be revisited by taking into account the observational errors. Such a problem was approached by means of numerical simulations in Paper I. We found that under certain circumstances, the χ^2 hypersurface is characterised by two or more relative minima. In these cases, the best-model is usually representative of the actual magnetic configuration, but not always. Sometimes the true magnetic topology is best described by the model corresponding to a secondary minimum, or, in the most extreme cases, it is not recovered at all by the inversion algorithm. The occurrence of multiple solutions (that is, several relative minima characterised by similar values for the χ^2 – which ought not be confused with the degeneracy of the magnetic configuration discussed in Sect. 3) is related to the magnitude of the observational errors, but depends also on the region of the parameter space where the magnetic configuration is located. We will shortly see how this reflects on the analysis of the magnetic configuration of β CrB.

A modelling which includes observations of BBLP requires one to introduce a larger number of approximations and free parameters than the analysis of the magnetic quantities derived from Stokes I and V profiles. In particular, the observations of BBLP are more sensitive to the possible presence of abundance patches at the surface of the star. On the contrary, when measuring I and V profiles, it is possible to select spectral lines whose shape does not appear affected by an abundance modulation of the element from which they originate. Therefore, we decided to follow a two-step procedure. First we modelled the observations of longitudinal field, crossover, square field and field modulus (together with the explicit constraints to $v_e \sin i$ and R_*). Then we repeated the calculations by including the observations of BBLP, and we compared the results.

Even by neglecting the observations of BBLP, it is clear that the simple dipole field is not sufficient to describe the magnetic configuration of β CrB. In Bagnulo et al. (1999a) we found that

the observations of longitudinal field, crossover and square field could be well explained by a dipole field, but the best-model could not account for the curve of field modulus. By applying the new technique presented in this paper, that is, by explicitly including the field modulus in the inversion algorithm, we found that the best-fit to the magnetic data has a reduced $\chi^2 = 7.7$. The fact that the magnetic morphology of β CrB cannot be approximated by a dipole field has been well-known for a long time (see, e.g., Stift 1975). The two extrema of the curve of field modulus are not in phase with the extrema of the curve of longitudinal field, but almost in phase quadrature (see Fig. 2). This feature cannot be reproduced with a simple dipolar field (Landolfi et al. 1997; Mathys et al. 1997).

The situation radically improves (even too much!) when including a quadrupolar component. We found *four* models, with reduced $\chi^2 \simeq 1.4 - 1.8$, that account for the curves of longitudinal field, crossover, square field and field modulus (the predictions of the best one are shown in Fig. 2 with dotted lines). Very few characteristics are common to these models: a low value for the inclination angle i and a value for β near 90° , which also explains why the remaining parameters are so scattered: the observer sees only a limited fraction of the stellar surface, as the rotation axis is almost pole-on.⁵ This greatly weakens the constraints to the magnetic morphology, especially because the measurements derived via Stokes I and V are basically sensitive to the modulus and the longitudinal component of the magnetic field. It is clear that the observations of BBLP, sensitive to the transverse component of the field, may be of great help to constrain the magnetic configuration of the star, although, as we shall discuss in Sect. 4.3, their interpretation requires some caution.

As explained in Sect. 3, when considering the observations of BBLP, we have to introduce a number of additional parameters. Four of them (α , Θ , P_Q^{int} , P_U^{int}) are free, that is, their values are recovered by the inversion algorithm. Three parameters (η_0 , a , b) are treated as fixed.

The choice of η_0 and a depends on which features we believe should pertain to the ‘average’ line that we deem as representative of the stellar spectrum. One could assume that the ‘average’ line should simply account for the magnetic observations, and select its parameters in order to produce the best-fit to the BBLP. We soon realised that this approach would lead to some clashing inconsistency, since the best-fits were obtained for $\eta_0 < 1$: a line characterised by such a small strength would in fact be invisible in the spectrum, which by contrast appears to be crowded of strong lines (see, e.g., Hiltner 1945). We thus decided to follow a more realistic approach, that is, to fix η_0 and a such that the resulting line be representative of the observed stellar spectrum, and account for the overall line-blocking factor, ξ , in the wavelength region of the observations of BBLP (ξ was mea-

⁵ These features of the magnetic morphology of β CrB, that is, a rotation axis almost pole-on and the dipolar axis almost perpendicular to the rotation axis, are also common to the best pure dipole model, and were found in previous works by several authors, e.g., Wolff & Wolff (1970), Stift (1975).

sured at 4200 Å by Wolff 1967 as 0.26). At the same time, the line parameters to be adopted should also be consistent with our assumption that the spectral lines are not blended. Under the hypothesis of Milne-Eddington atmosphere we calculated, by numerical integration over the stellar disk, the line profile for several combinations of η_0 , a , and β_P . We concluded that the appropriate value of η_0 for the ‘average’ line should be comprised in the interval $2 \lesssim \log \eta_0 \lesssim 3$. *A posteriori* we found that both the observed line-blocking factor and BBLP could be best explained with the values $\eta_0 = 300$ and $a = 0.05$. However, it should be noted that the model predictions for the observed BBLP are almost independent of the precise value of η_0 within a range of one order of magnitude.

An estimate for the conversion factor b can be obtained from Eq. (12) by recalling

$$\Delta\nu_D = \frac{1}{\lambda_0} \sqrt{\frac{2k_B T_{\text{eff}}}{m_p A} + w^2}, \quad (21)$$

where k_B is the Boltzmann constant, m_p the proton mass, A the atomic weight, w the microturbulent velocity, and $\lambda_0 \simeq 4200$ Å. By taking $T_{\text{eff}} = 7750$ K, $0.0 \leq w \leq 2.5$ km s⁻¹, and by assuming that the spectrum of β CrB is dominated by iron peak element lines, we obtain $b \simeq 2500 - 5000$ G. We carried out our analysis by adopting various values of b within this range. Here we describe the results corresponding to the two boundary values. (For intermediate values of b we obtained results consistent with those illustrated below.)

By setting $b = 2500$ G, the parameters of the best-model are

$$\begin{aligned} i &= 168^\circ \pm 1^\circ \\ \Theta &= 124^\circ \pm 2^\circ \\ \beta &= 88^\circ \pm 1^\circ \\ f_0 &= 5^\circ \pm 2^\circ \\ \beta_1 &= 12^\circ \pm 1^\circ \\ \beta_2 &= 79^\circ \pm 1^\circ \\ \gamma_1 &= 350^\circ \pm 5^\circ \\ \gamma_2 &= 331^\circ \pm 1^\circ \\ B_d &= 12165 \pm 55 \text{ G} \\ B_q &= 14420 \pm 70 \text{ G} \\ v_e &= 8.4 \pm 0.6 \text{ km s}^{-1} \\ \alpha &= 8.3 \times 10^{-3} \pm 0.4 \times 10^{-3} \\ P_Q^{\text{int}} &= 4.1 \times 10^{-4} \pm 0.5 \times 10^{-4} \\ P_U^{\text{int}} &= 0.6 \times 10^{-4} \pm 0.3 \times 10^{-4}, \end{aligned} \quad (22)$$

the associated values for $v_e \sin i$ and R_* are 1.8 ± 0.2 km s⁻¹ and $3.1 \pm 0.2 R_\odot$, respectively, and the value of the reduced χ^2 is 2.0. The model yields an average line-blocking factor of 0.26. The zero phase point refers to J.D. = 2450011.06, and the fits are shown with dashed lines in Fig. 2.

This model is unique, in the sense that the secondary minima of the χ^2 hypersurface either give for the line-blocking factor a value less than a half of the observed one, or correspond to a much larger value of the reduced χ^2 ($\gtrsim 3.0$). However, this model is not consistent with any of the four models recovered by neglecting the observations of BBLP.

By setting $b = 5000$ G, the absolute minimum of the χ^2 hypersurface corresponds to a set of parameters similar to that

of Eq. (22). On the one hand, this somehow strengthens the reliability of that model. On the other hand, the solution is no longer unique. A secondary minimum is found for the following set of parameters

$$\begin{aligned} i &= 162^\circ \pm 1^\circ \\ \Theta &= 35^\circ \pm 2^\circ \\ \beta &= 93^\circ \pm 1^\circ \\ f_0 &= 0^\circ \pm 2^\circ \\ \beta_1 &= 40^\circ \pm 2^\circ \\ \beta_2 &= 114^\circ \pm 2^\circ \\ \gamma_1 &= 143^\circ \pm 2^\circ \\ \gamma_2 &= 35^\circ \pm 1^\circ \\ B_d &= 8810 \pm 370 \text{ G} \\ B_q &= 15145 \pm 90 \text{ G} \\ v_e &= 9.1 \pm 0.7 \text{ km s}^{-1} \\ \alpha &= 8.2 \times 10^{-3} \pm 0.8 \times 10^{-3} \\ P_Q^{\text{int}} &= 2.0 \times 10^{-4} \pm 0.3 \times 10^{-4} \\ P_U^{\text{int}} &= 0.4 \times 10^{-4} \pm 0.3 \times 10^{-4}. \end{aligned} \quad (23)$$

The associated values for $v_e \sin i$ and R_* are 2.8 ± 0.4 km s⁻¹ and $3.3 \pm 0.4 R_\odot$, respectively, and the value of the reduced χ^2 is 2.5. The fits are shown with solid lines in Fig. 2. The morphology of this model, which predicts an average line-blocking factor of 0.22, is similar to the *best* of the four models obtained by neglecting the observations of BBLP (the main difference is that the model of Eq. (23) predicts a slightly different orientation of the quadrupolar component, and an overall magnetic strength about 25 % larger than what predicted by the best model obtained without BBLP).

Note that both models of Eqs. (22) and (23) are characterised by relatively high values for the reduced χ^2 and very small values for the parameter errors. This latter feature indicates that the χ^2 hypersurface is very steep in correspondence to the minimum. It would be misleading to interpret this in terms of a high precision result. On the contrary, this seems rather a clue to the presence of a magnetic configuration more complex than a dipole plus quadrupole. In the following we will examine this hypothesis in more detail.

4.3. Discussion

Inspection of the fits in Fig. 2 shows the presence of some systematic effects.

In the vicinity of the minimum of the longitudinal field, the measured field is more negative than predicted by the model. This discrepancy is stronger in the models obtained taking into account the observations of BBLP (dashed and solid lines) than in the one obtained neglecting them (dotted lines). Therefore, for the former two models, this systematic discrepancy might partly be an artifact of the modelling due to the presence of element abundance patches (we will come back later on this point). On the other hand, one could interpret this discrepancy as due to a magnetic morphology even more complex than what can be described by means of a second-order multipolar expansion.

One could also suspect an overestimate of the adopted determinations of longitudinal field (altogether, the observations of other authors would be better reproduced by our models). In

any case, the points near the minimum of the curve showing the largest deviations are few, so that their weight is low compared to the whole set of observations. Indeed, we found similar modelling results even by neglecting them.

It is also evident that many determinations of square field are below the model predictions. This seems to be intrinsic to the way the various magnetic quantities are derived, rather than to indicate a shortcoming of the model. Plain comparison of the values of the longitudinal field, of the field modulus, and of the square field throughout the rotation cycle of stars for which these three magnetic quantities have been repeatedly determined shows that for many of them, the derived values are at the limit of mutual inconsistency, in the sense that the inequality

$$\langle \mathcal{B} \rangle^2 + \langle \mathcal{B}_z \rangle^2 \leq \langle \mathcal{B}^2 + \mathcal{B}_z^2 \rangle^{1/2}$$

is often only marginally satisfied (Mathys et al. in preparation). Although no definite incompatibility has been found for any star, the fact that in many instances the square field hardly exceeds the sum of the square of the longitudinal field and of the square of the field modulus suggests that the technique used to derive the magnetic quantities tends to somewhat underestimate the former with respect to the latter two (or conversely, to overestimate one or both of the latter two with respect to the former). The error, if real, is rather small compared to the values of the corresponding magnetic quantities, but it may be sufficient to account for the kind of difficulty which appears here when trying to use them all simultaneously to establish a best magnetic model.

The determinations of mean field modulus are definitely better reproduced by the model obtained without taking into account the observations of BBLP (dotted lines) than by the models of Eq. (22) or (23). Similarly to what is discussed for the longitudinal field, this suggests either that the magnetic structure of β CrB is more complex than a dipole plus quadrupole, or that BBLP introduces some artifact in the modelling.

In fact, the observations of BBLP are well reproduced by both models of Eqs. (22) and (23). Nevertheless, a few comments are still needed.

One of the problems to be addressed is related to the presence of a companion. Assuming that the radiation arising from the companion is not polarised, the binarity simply causes a dilution of the signal of BBLP by a factor $\lesssim 20\%$, and introduces a minor indetermination in the value of the line-blocking factor ξ ($\simeq 20\%$ of the difference between the line-blocking factors of the two stars). From a qualitative point of view, it can be expected that the dilution effect of the BBLP signal basically affects the only parameter α . Since the line-blocking factor

$$\xi = \alpha \int_0^{2\pi} d\chi \int_0^{\pi/2} d\theta c(\theta; u) \int_{\text{line}} dv [1 - i(\theta, \chi)]$$

is almost constant with the rotational phase, and much less than unity, the parameter α in the numerator of the first terms in the r.h.s. of Eqs. (8) acts in practice as a scaling factor – which is just the effect due to the dilution of the signal. Such expectations have been verified by applying again the inversion procedure, with the BBLP measurements artificially multiplied by a factor

1.2. For any given set of η_0 , a , b we recovered magnetic configurations quite similar to the previous ones, except for the value of α .

The assumption that the observed BBLP is due to a single ‘average’ line (or equivalently, to N identical, unblended lines) may look questionable for a star like β CrB, whose spectrum is crowded of lines and undoubtedly contains several blends. This problem was studied by Bagnulo et al. (1999b) through the comparison with realistic synthetic spectra. In fact, they found that the behaviour of BBLP as a function of rotational phase, for a given magnetic configuration, is not strongly affected by the above assumption. Therefore, we do not regard this approximation as a major problem, all the more so because the modelling results are based not only on BBLP observations, but also on other kinds of constraints.

The last point to be addressed is related to the possible presence of abundance patches at the surface of the star. Leroy et al. (1995) showed that abundance variations were not sufficient to explain the departures of the observed BBLP from what expected for a simple dipolar configuration. Furthermore, the spectral lines of β CrB do not display strong variations of equivalent width (Mathys 1991). As the rotation axis has a small inclination to the line of sight, this does not rule out the possible existence of pretty large abundance inhomogeneities. Such inhomogeneities, if present, would primarily appear as rotating features permanently within sight on the stellar disk, and as such they might introduce a modulation of the BBLP signal sufficient to weaken the full validity of our interpretation. For instance, they could be responsible for the partial discrepancy between model predictions and observations of mean field modulus and longitudinal field.

According to the above discussion, one could regard the model of Eq. (22), which is not consistent with any of the models recovered independently of the observations of BBLP, as an artifact of the modelling due to the presence of abundance patches. In addition, note that the value of $v_e \sin i$ associated to the model of Eq. (22) is marginally inconsistent with the estimate of Wade (1996), and the interstellar polarisation may look suspiciously high for a star only 35 pc away. By contrast the model of Eq. (23), which in fact is *similar* to the best of the models obtained by neglecting the BBLP, seems more reliable.

The magnetic maps corresponding to the models of β CrB given in Eqs. (22) and (23) are shown in Figs. 3 and 4, respectively. Both figures are organised in a similar way. The modulus of the magnetic field is visualised by means of different colours, with contour lines 1 kG apart. (The legend is shown in the left-middle panels.) The direction of the magnetic field is represented by unit vectors, drawn in black or gray according to their outward or inward orientation, respectively.

The upper four panels show the configuration of the star as seen from the observer. In Fig. 3 the rotation axis is tilted at an angle $i = 168^\circ$ and its azimuth, $\Theta = 124^\circ$, is counted counterclockwise from the direction oriented toward the top of the page. In Fig. 4 the rotation axis is tilted at an angle $i = 162^\circ$ and its azimuth is $\Theta = 35^\circ$. (We recall, however, that the values Θ_0 and $\Theta_0 + 180^\circ$ cannot be distinguished.)

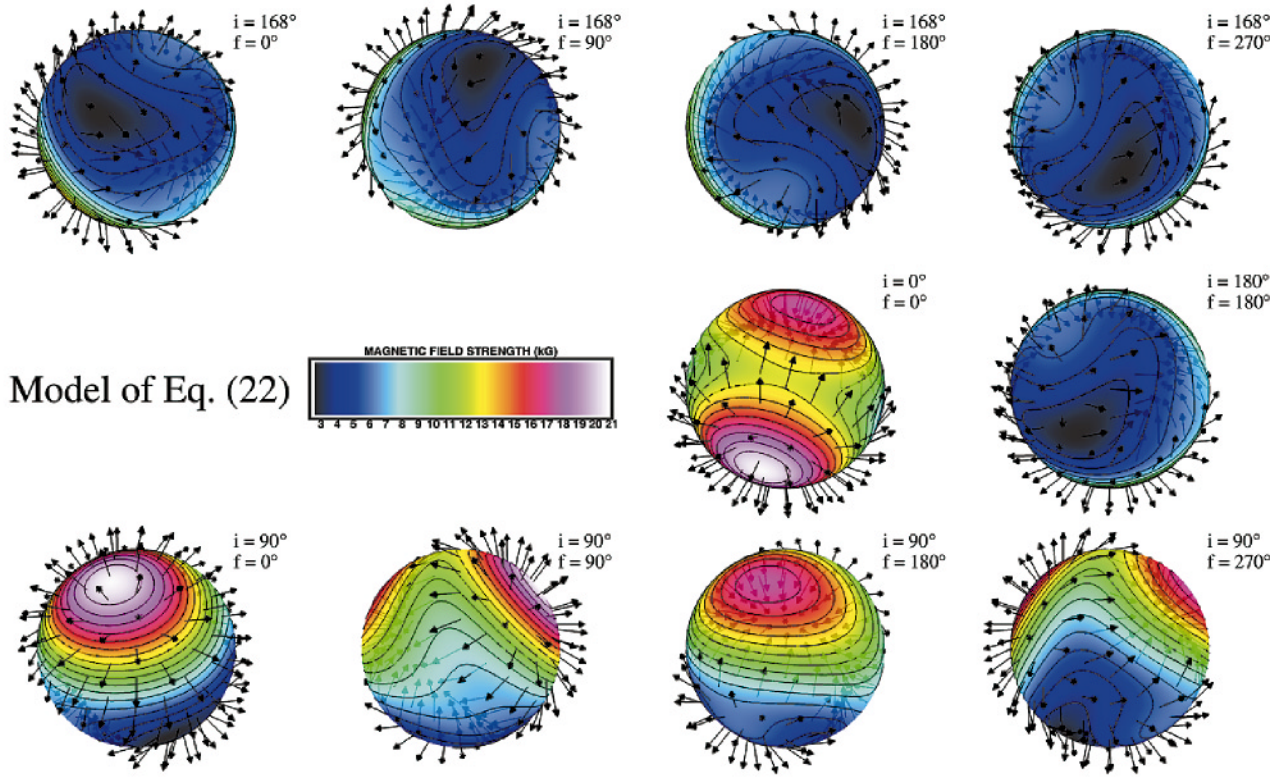


Fig. 3. The magnetic configuration of β CrB according to the model of Eq. (22). The figure is explained the text

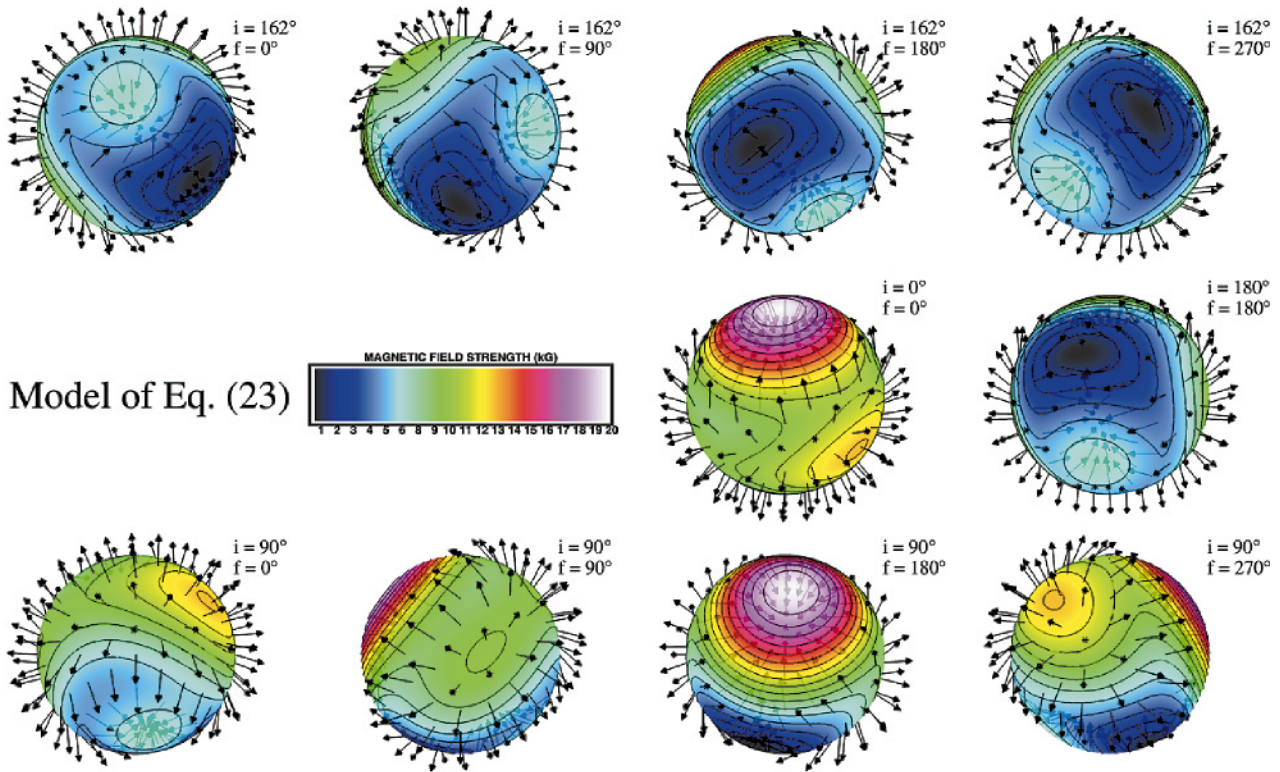


Fig. 4. The magnetic configuration of β CrB according to the model of Eq. (23). The figure is explained the text

The remaining panels display the magnetic configuration over the entire stellar surface. The rotation axis is taken as preferred direction. The two middle panels (beside the legend) show the magnetic structure as seen from the North, and from the South rotation pole ($i = 0^\circ$ and $i = 180^\circ$, respectively). The four bottom panels show the star with the rotation axis perpendicular to the line of sight ($i = 90^\circ$), at four different rotation phases specified in the figure. The visible rotation pole is arbitrarily set toward the top of the page ($\Theta = 0^\circ$).

The magnetic maps clearly show that, according to both models, the morphology of β CrB exhibits magnetic patches of strong field right on the side of the stellar surface that is *not* visible to the observer. A similar result was found in a previous work for HD 119419 (Bagnulo & Landolfi 1999). It would probably be naïve to believe that this represents a physical reality. It rather suggests that the magnetic morphology of β CrB (as well as that of other CP stars) is more complex than what can be represented by means of a second-order multipolar expansion. The strong field gradients in the non visible stellar hemisphere, especially those of the model of Eq. (22), look like a mathematical artifact of our method, which is ‘forced’ to represent the actual magnetic structure with an insufficient number of free parameters. The same remarks are also suggested by the relatively high value of the reduced χ^2 of the best-models, and by the suspiciously low values for the errors associated to the model parameters (see Sect. 4.2). However, it makes sense to suppose that the magnetic morphology as described over the visible stellar hemisphere is similar to the actual one. New determinations of the observable quantities obtained via higher-resolution spectra and exploitation of additional constraints derived from the consideration of line profile moments beyond the second order will certainly help to obtain less ambiguous results.

5. Conclusions

We have presented a method to recover the magnetic morphology of CP stars from the modelling of mean longitudinal field, crossover, mean square field, mean field modulus, and broadband linear polarisation observations, under the assumption of a centred dipole plus non-linear quadrupole field. Constraints to the stellar radius and the projected equatorial velocity are also explicitly taken into account.

We have applied the method to the well-known magnetic star β CrB. This choice is appropriate in the sense that β CrB is the only object for which observations of all the magnetic quantities are available. On the other hand, the particular orientation of the star is not fully suitable to obtain unambiguous conclusions. Since the rotation axis is almost pole-on, the observer sees only about half of the entire stellar surface throughout the rotation cycle, which weakens the constraints to the magnetic morphology. In fact, we found two different magnetic configurations that can explain the observations of all the magnetic quantities, and account for the values of the stellar radius, the projected equatorial velocity, and the line-blocking factor. In both cases, the magnetic morphology exhibits strong field gradients on the side of the stellar hemisphere which is not visible to the ob-

server. This suggests that the magnetic configuration of β CrB could be even more complicated than what can be described by a second-order multipolar expansion. The modelling may be revisited either when new high-quality data become available, or by taking into account additional magnetic parameters that could be determined from further analysis of the line profiles. Nevertheless, ultimately, any model that is derived will have to be used to build synthetic spectra for comparison with the spectra observed in the various Stokes parameters, as a consistency check in order to validate (and possibly refine) the models and to establish that the derived magnetic morphology is fully compatible with the existing observational constraints.

Acknowledgements. Stefano Bagnulo has been supported by the Austrian *Fonds zur Förderung der Wissenschaftlichen Forschung*, project P12101-AST.

References

- Babcock H.W., 1947, ApJ 105, 105
- Babcock H.W., 1958, ApJS 3, 141
- Babcock H.W., 1960, ApJ 132, 521
- Bagnulo S., Landi Degl’Innocenti E., Landolfi M., Leroy J.-L., 1995, A&A 295, 459
- Bagnulo S., Landi Degl’Innocenti M., Landi Degl’Innocenti E., 1996, A&A 308, 115
- Bagnulo S., Landolfi M., 1999, A&A 346, 158
- Bagnulo S., Landolfi M., Landi Degl’Innocenti M., 1999a, A&A 343, 865
- Bagnulo S., Stift M.J., Leone F., Kurtz D.W., Martinez P., 1999b, In: Nagendra K.N., Stenflo J.O. (eds.) *Solar Polarization*. Kluwer, Dordrecht, p. 459
- Bevington P.R., 1969, *Data reduction and error analysis for the physical sciences*. McGraw-Hill, New York
- Borra E.F., Landstreet J.D., 1980, ApJS 42, 421
- Hensberge H., van Rensbergen W., Goossens M., Deridder G., 1979, A&A 75, 83
- Hiltner W.A., 1945, ApJ 102, 43
- Hubrig S., North P., Mathys G., 2000, ApJ (in press)
- Landi Degl’Innocenti M., Calamai G., Landi Degl’Innocenti E., Patriarchi P., 1981, ApJ 249, 228
- Landolfi M., Landi Degl’Innocenti E., 1982, Solar Phys. 78, 355
- Landolfi M., Landi Degl’Innocenti E., Landi Degl’Innocenti M., Leroy J.-L., 1993a, A&A 272, 285
- Landolfi M., Landi Degl’Innocenti E., Landi Degl’Innocenti M., Leroy J.-L., Bagnulo S., 1993b, In: Dworetzky M.M., Castelli F., Faraggiana R. (eds.) *Peculiar versus normal phenomena in A-type and related stars*. IAU Colloquium No. 138, ASP Conference Series vol. 44, p. 305
- Landolfi M., Bagnulo S., Landi Degl’Innocenti M., Landi Degl’Innocenti E., Leroy J.-L., 1997, A&A 322, 197
- Landolfi M., Bagnulo S., Landi Degl’Innocenti M., 1998, A&A 338, 111 (Paper I)
- Landstreet J.D., 1992, A&AR 4, 35
- Leroy J.-L., 1962, Ann. Astrophys. 25, 127
- Leroy J.-L., 1995a, A&AS 114, 79
- Leroy J.-L., 1995b, In: Mein N., Sahal-Bréchet S. (eds.) *La Polarimétrie, outil pour l’étude de l’activité magnétique solaire et stellaire*. Observatoire de Paris
- Leroy J.-L., Landolfi M., Landi Degl’Innocenti M., et al., 1995, A&A 301, 797

- Mathys G., 1991, A&AS 89, 121
Mathys G., 1994, A&AS 108, 547
Mathys G., 1995a, A&A 293, 733
Mathys G., 1995b, A&A 293, 746
Mathys G., 1999, In: Nagendra K.N., Stenflo J.O. (eds.) Solar Polarization. Kluwer, Dordrecht, p. 489
Mathys G., Hubrig S., 1997, A&AS 124, 475
Mathys G., Hubrig S., Landstreet J.D., Lanz T., Manfroid J., 1997, A&AS 123, 353
Michaud G., Mégessier C., Charland Y., 1981, A&A 103, 244
North P., Carquillat J.-M., Ginestet N., Carrier F., Udry S., 1998, A&AS 130, 223
Preston G.W., Sturch C., 1967, In: Cameron R.C. (ed.) The Magnetic and Related Stars. Mono Book Corporation, Baltimore, p. 111
Romanyuk I.I., 1986, In: Cowley R., Dworetzky M., Megessier C. (eds.) Upper Main Sequence Stars with Anomalous Abundances. ASSL series vol. 125, Reidel, Dordrecht, p. 359
Shurcliff W.A., 1962, Polarized light. Harvard University Press, Cambridge
Stift M.J., 1975, MNRAS 172, 133
Tokovinin A., 1985, A&AS 61, 483
Vogt S.S., Tull R.G., Kelton P.W., 1980, ApJ 236, 308
Wade G.A., 1996, In: Glagolevskij Yu.V., Romanyuk I.I. (eds.) Stellar Magnetic Fields. Moscow, p. 55
Wade G.A., Elkin V.G., Landstreet J.D., Romanyuk I.I., 1997, MNRAS 292, 748
Wade G.A., Donati J.-F., Mathys G., Piskunov N., 1998, Contrib. Astron. Obs. Skalnaté Pleso 27, 344
Wolff S.C., 1967, ApJS 15, 21
Wolff S.C., 1978, PASP 90, 412
Wolff S.C., Wolff R.J., 1970, ApJ 160, 1049